

Three Phases in the 3D Abelian Higgs Model with Nonlocal Gauge Interactions

Shunsuke Takashima,¹ Ikuo Ichinose,¹ Tetsuo Matsui,² and Kazuhiko Sakakibara³

¹*Department of Applied Physics, Nagoya Institute of Technology, Nagoya, 466-8555 Japan*

²*Department of Physics, Kinki University, Higashi-Osaka, 577-8502 Japan*

³*Department of Physics, Nara National College of Technology, Yamatokohriyama, 639-1080 Japan*

(November 6, 2018)

We study the phase structure of the 3D nonlocal compact U(1) lattice gauge theory coupled with a Higgs field by Monte Carlo simulations. The nonlocal interactions among gauge variables are along the temporal direction and mimic the effect of local coupling to massless particles. In contrast to the 3D local abelian Higgs model having only the confinement phase, the present model exhibits the confinement, Higgs, and Coulomb phases separated by three second-order transition lines emanating from a triple point. This suggests that electron fractionalization phenomena in strongly-correlated electron systems may take place not only in the Coulomb phase but also in the Higgs phase.

Some recent experiments in strongly-correlated electron systems indicate breakdown of Landau Fermi liquid theory. Also, for certain class of quantum phase transitions, it is argued that Ginzburg-Landau theory is not applicable [1]. In these cases, the crucial point is the change of particle picture: quasiparticles are no longer electrons but certain new objects carrying fractional/exotic quantum numbers. These objects may be “constituents” of the original electrons. For example, each electron in a high- T_c cuprate may be a composite of a holon and a spinon. Anderson [2] argued that the anomalous properties of the normal state may be understood by regarding these holons and spinons as quasiparticles. This phenomenon of dissociation of electrons is called the charge-spin separation (CSS). Another example is Jain’s composite-fermion picture of the fractional quantum Hall effect (FQHE) [3], where each electron is viewed as a composite of a so-called composite fermion and fictitious magnetic fluxes. Jain argued that when these fluxes cancel the external magnetic field partly, the FQHE is understood as the integer QHE of composite fermions in the residual field.

To investigate these possibilities of fractionalization of electrons, knowledge and methods of gauge theory are useful. In fact, in path-integral formalism, one can introduce a U(1) gauge field as an auxiliary field that binds the constituents of each electron, and study the dissociation phenomena as a confinement-deconfinement phase transition (CDPT) of this gauge dynamics. For the CSS, by starting from the $t - J$ model and using the hopping expansion, we have argued that a CDPT takes place at certain critical temperature $T = T_{\text{CSS}}$ and the CSS is possible *below* T_{CSS} [4]. For the FQHE, by introducing a fermion (we called it chargon) for a composite fermion and a boson (fluxon) for fluxes, we have again supported the CDPT [5] at $T = T_{\text{PFS}}$ below which chargons and fluxons separate. We called this phenomenon particle-flux separation (PFS). Furthermore, when fluxons Bose condense, Jain’s idea of FQHE is realized.

For the three-dimensional (3D) compact U(1) gauge

system with local interactions *without coupling to matter fields*, Polyakov showed that the system stays always in the confinement phase due to the instanton condensation [6]. However, the issue of whether a CDPT is possible for a 3D (spatial 2D at $T = 0$)U(1) gauge system *with matter fields* is still controversial [7], mainly due to the lack of convincing methods for investigating a system with *massless(gapless)* matter fields whose effect is crucial for the phase structure. In the previous Letter [8] we introduced a 3D compact U(1) pure lattice gauge theory with *nonlocal gauge interactions* along the temporal direction which simulate the effect of gapless matter fields in the parity-symmetric phase [9]. By numerical simulations, we found that the CDPT occurs at a certain gauge coupling. The existence of the deconfinement phase supports the fractionalization phenomena like the CSS and PFS.

To push forward this gauge theoretical approach in more realistic manner, one needs to include another matter field, i.e., a Higgs field, coupled to the gauge field locally. Actually, in the slave-boson (SB) t-J model, there appear fermionic spinons, bosonic holons, and a U(1) gauge field. In the flux state of the mean-field theory [10], spinons are regarded as massless Dirac fermions in a parity doublet. Such a spin system is studied also as an algebraic spin liquid [11]. To examine the effect of these Dirac fermions on the phase structure, etc., we perform path integration over the fermions formally, and approximate the resulting fermionic determinant by the nonlocal gauge interactions introduced in Ref. [8]. To describe the bosonic holons one may introduce a U(1) Higgs field with the fundamental charge, its amplitude being fixed as $\sqrt{\delta}$, where δ is the holon density. In the chargon-fluxon model of the FQHE, integration over fermionic chargons certainly generate nonlocal gauge interactions, and bosonic fluxons may be treated as a Higgs field coupled to this gauge field.

In this Letter we extend the previous study [8] by coupling a U(1) Higgs field to the gauge field locally, and investigate the phase structure of this nonlocal Abelian Higgs model (AHM). Since the ordinary (local) 3D AHM

in the London limit (no radial fluctuations) has only the confinement phase [12,13], it is interesting to see if the nonlocal interactions among the gauge field are capable of generating a phase transition into the Higgs phase. In the SB t - J model and an algebraic spin liquid with doped holes, the possible Higgs phase implies a superconducting state. In the FQHE regime, the Higgs phase is indispensable to achieve Jain's idea [3] since a condensation of fluxons is necessary to cancel the uniform external magnetic field partly.

We consider the nonlocal AHM defined on the cubic lattice of the size $V = N_0 N_1 N_2$ with the periodic boundary condition. The compact $U(1)$ gauge field $U_{x\mu} = \exp(i\theta_{x\mu})$ ($-\pi < \theta_{x\mu} \leq \pi$) is put on each link $(x, \mu) \equiv (x, x + \hat{\mu})$ ($\mu = 0, 1, 2$), and the Higgs field $\phi_x = \exp(i\varphi_x)$ ($-\pi < \varphi_x \leq \pi$) on each site x . The partition function Z is given by

$$Z = \int \prod_{x,\mu} dU_{x\mu} \prod_x d\phi_x \exp(A), \quad A = A_G + A_H. \quad (1)$$

A_G is the gauge part of the gauge-invariant action A [14],

$$A_G = g \sum_x \sum_{i=1}^2 \sum_{\tau=1}^{N_0} c_\tau (V_{x,i,\tau} + \bar{V}_{x,i,\tau}) + A_S,$$

$$V_{x,i,\tau} = \bar{U}_{x+\tau\hat{0},i} \prod_{k=0}^{\tau-1} [\bar{U}_{x+k\hat{0},0} U_{x+\hat{i}+k\hat{0},0}] U_{xi},$$

$$A_S = g\lambda \sum_x (\bar{U}_{x2} \bar{U}_{x+\hat{2},1} U_{x+\hat{1},2} U_{x1} + \text{c.c.}), \quad (2)$$

where g is the (inverse) gauge coupling constant, $V_{x,i,\tau}$ is the product of $U_{x\mu}$ along the rectangular $(x, x + \hat{i}, x + \hat{i} + \tau\hat{0}, x + \tau\hat{0})$ of the size $(1 \times \tau)$ in the $(i-0)$ plane ($i = 1, 2$), and c_τ is the "nonlocal coupling constant". A_S is the spatial single-plaquette coupling of $U_{x\mu}$'s. A_H is the local Higgs action,

$$A_H = \kappa \sum_{x,\mu} (\bar{\phi}_{x+\hat{\mu}} U_{x\mu} \phi_x + \text{c.c.}), \quad (3)$$

where κ is the Higgs coupling. In the SB t - J model, $\kappa \propto \delta$ as explained.

In the previous study [8] of the pure gauge system ($\kappa = 0$), we considered (i) power-law decay $c_\tau = 1/\tau$ simulating the effect of massless relativistic matter fields and (ii) exponential decay $c_\tau = \exp(-m\tau)$ mimicking massive matter fields. We found a second-order CDPT for the case (i); the critical coupling is $g_c = 0.10 \sim 0.12$ for $\lambda = 1$, while no CDPT for the case (ii). We also studied (iii) no decay case $c_\tau = \text{const}$ for nonrelativistic fermions in which the CDPT was observed at very small coupling like $g_c = 0.03$ for $V = 24^3$. Then one can naturally expect that if the Higgs transition exists in the power-law decay case, it also exists in the no-decay case.

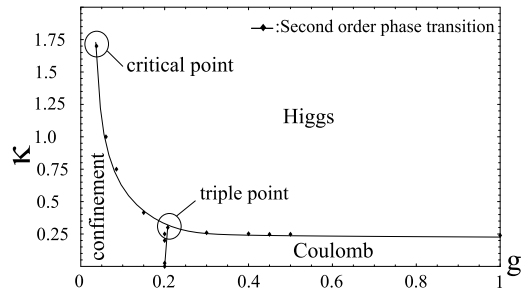


FIG. 1. Phase diagram of the 3D nonlocal AHM. There are three transition lines, which are determined by the location of the peak of C for $N = 16$.

In the following numerical studies of the gauge model Eq.(1), we concentrate on the power-law decay case (i) with $\lambda = 1$ on the cubic lattice $V = N^3$ up to $N = 24$. We first measure the "internal energy" E and the "specific heat" C defined as

$$E \equiv -\frac{1}{V} \langle A \rangle, \quad C \equiv \frac{1}{V} \langle (A - \langle A \rangle)^2 \rangle. \quad (4)$$

In Fig.1 we present the phase diagram in the g - κ plane determined by the measurement of E and C . There are three transition lines separating three phases which we call the confinement, Higgs, and Coulomb phases. (We shall identify each phase later by measuring the instanton density and the Higgs boson mass.)

Let us first consider the confinement-Coulomb transition line. It includes the CDPT at $\kappa = 0$ previously found in Ref. [8]. Thus the deconfinement phase observed in Ref. [8] is identified as the Coulomb phase. We measured E and C along a fixed κ and found that E exhibits no hysteresis and the peak of C develops as the system size N^3 increases just as in the $\kappa = 0$ case [8]. These are the typical signals of a second-order phase transition. We note that the location of the peak of C shifts into the smaller g (higher- T) direction for larger N , just the opposite to the case of local interaction. It is because the new gauge interactions are introduced as N increases, and these terms favor to suppress fluctuations of $U_{x\mu}$ [8].

Next, let us consider the Coulomb-Higgs transition. In Fig.2 we present C vs. κ for $g = 1.0$. As N increases,

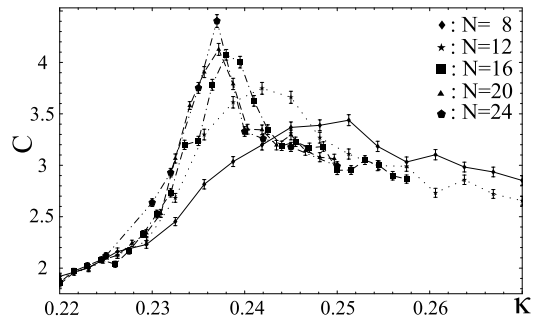


FIG. 2. Specific heat C vs. κ for $g = 1.0$. The peak develops as N increases.

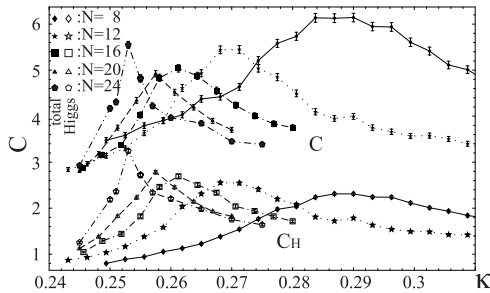


FIG. 3. Total specific heat C (upper) and its Higgs part C_H (lower) vs. κ for $g = 0.3$.

the peak of C also develops. Again, the location of the peak shifts to smaller κ because of the nonlocal action A_G . To confirm that this transition is of second order, we apply the finite-size scaling hypothesis [15] to C of Fig.2. We fit C as a function of N and $\epsilon \equiv (\kappa - \kappa_\infty)/\kappa_\infty$, where κ_∞ is the critical Higgs coupling at $N \rightarrow \infty$, in the form of $C_N(\epsilon) = N^{\sigma/\nu} \phi(N^{1/\nu} \epsilon)$ with certain scaling function $\phi(x)$. We get a quite good fitting for $N = 8 \sim 24$ with $\nu = 0.75$, $\kappa_\infty = 0.23$ and $\sigma = 0.12$.

In Fig.3 we present C for a smaller value of g , $g = 0.3$. As N increases from $N = 8$ to 20, C gets sharper but the height of its peak becomes lower. To understand this interesting behavior, we measured the “specific heats” of the gauge part and Higgs part, $C_O = \langle (A_O - \langle A_O \rangle)^2 \rangle / V$ ($O = G$ and H), separately [13]. C_H in Fig.3 has a developing peak as in the usual second-order phase transition. On the other hand, both C_G and the cross term, $C - C_H - C_G$, are smooth and reduce as N increases. As explained above, the gauge specific heat C_G has the peak which shifts to left (smaller g) for increasing N . Then the tail of C_G observed at a fixed g on the right of the confinement-Coulomb transition line reduces as N increases. This reduction gives rise to the above behavior of C in Fig.3 at $g = 0.3$ which is close enough to the transition line at $g \sim 0.20$ (See Fig.1). For larger $N (\geq 24)$, the peak of C starts to develop as it should be since the Higgs part, the relevant part of the Coulomb-Higgs transition, starts to dominate over C_G and the cross term.

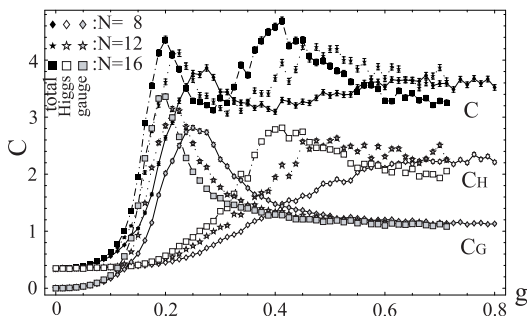


FIG. 4. Specific heat C, C_H, C_G vs. g for $\kappa = 0.25$. C has two peaks reflecting each peak of C_H and C_G .

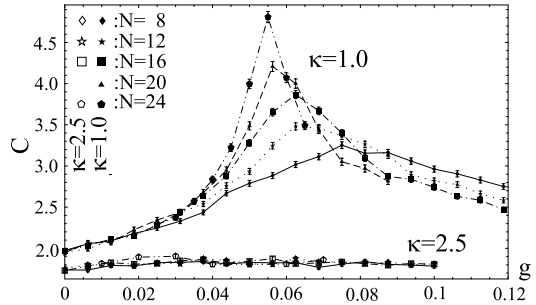


FIG. 5. C vs. g . For $\kappa = 1.0$, C has a peak that develops as N increases. For $\kappa = 2.5$, C has no peak.

Near the triple point, both C_G and C_H are relevant. In Fig.4 we present C vs. g for $\kappa = 0.25$. We choose $\kappa = 0.25$ as a horizontal line because it crosses the two transition lines near the triple point. Each peak of C_G and C_H develops with N simultaneously as expected.

Next, let us consider the confinement-Higgs transition. In Fig.5 we present C vs. g for $\kappa = 1.0$. At $g = 0$, one can exactly integrate over $U_{x\mu}$ to obtain $Z = [I_0(2\kappa)]^{3V}$, where I_0 is the modified Bessel function. Thus Z is an analytic function of κ , showing that there are no transitions along the line $g = 0$. We measured E and C at several fixed κ 's by varying g to find that the signal of second-order phase transition is getting weaker as κ increases. The phase transition line seems to terminate at the critical point, the location of which is roughly estimated as $g = 0.03, \kappa = 1.75$. This critical point is viewed as a nonlocal version of the complementarity between the Higgs and confinement phases discussed in Ref. [16].

In order to characterize these three phases, let us calculate the instanton density ρ_x [17]. ρ_x is the strength of monopoles sitting on the site of the dual lattice $x + (\hat{1} + \hat{2} + \hat{3})/2$, which measures the disorderedness of gauge-field configurations. In Fig.6 we show the average density $\rho \equiv \langle |\rho_x| \rangle$ for $g = 0.1$ and $g = 0.5$. In Fig.6(a), ρ is fairly large at the small κ region, and as crossing the transition point, it decreases rapidly. In Fig.6(b), ρ is already very low even in the small κ 's, and it decreases further across the transition point. Such behavior of ρ and the general relations $\rho(\text{confinement}) > \rho(\text{Coulomb}) > \rho(\text{Higgs})$ lead us to identification of each phase as shown in Fig.1.

For the AHM, one may study vortices of the Higgs field and their trajectories which form closed loops or terminate at (anti-)instantons [18]. The confinement phase is a plasma phase of instantons [6], i.e., the CDPT is characterized by dissociations of instanton-anti-instanton dipoles connected by vortex lines into a system of instanton plasma [18]. In Fig.6 we also plot the density of isolated instantons ρ_{single} by subtracting the nearest-neighbor dipole instanton pairs in the temporal direction. Fig.6 clearly shows that ρ_{single} survives only in the confinement phase as it should be.

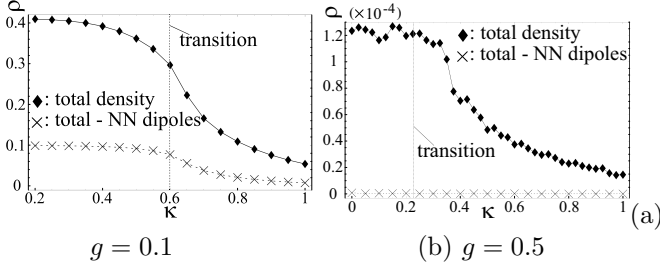


FIG. 6. Instanton density ρ for $N = 16$ vs. κ for (a) $g = 0.1$ and (b) $g = 0.5$. The crosses are the density ρ_{single} of isolated instantons. Dashed lines indicate the transition points. $\rho(g = 0.5)$ is smaller than $\rho(g = 0.1)$ by the factor $\sim 10^{-4}$.

Finally, let us consider masses of gauge-invariant operators. In Fig.7, we show the masses M_H (inverse correlation length) of $\text{Re}(\bar{\phi}_{x+\mu} U_{x\mu} \phi_x)$ and $\text{Im}(\bar{\phi}_{x+\mu} U_{x\mu} \phi_x)$ vs. κ for $g = 0.4$ [19]. The two M_H of Fig.7 exhibit the behavior across the transition point similar to that of the 4D local AHM [20]. We note that the 4D local AHM has a phase structure similar to the present model; three phases, a triple point and the complementarity. However at present, the confinement-Higgs transitions in the 4D AHM is believed to be of first order, which is in contrast to the present model.

In conclusion, we numerically studied the 3D nonlocal AHM and found that the nonlocal interactions generate all the known phases of gauge theory. As explained, the existence of the Higgs phase supports both the superconducting state of the $t-J$ model and the FQHE as electron fractionalization phenomena like CSS and PFS. In fact, the high- T_c cuprates near $T = 0$ enter into the superconducting state *above* some critical doping δ_c . This is interpreted in Fig.1 as entering into the Higgs phase as κ increases since $\kappa \propto \delta$. For a parity-preserving QED₃ coupled with a Higgs field, the result of the present model implies that a Higgs phase transition occurs for a sufficiently large number of fermion flavors since g is supposed to be proportional to the number of massless relativistic fermions.

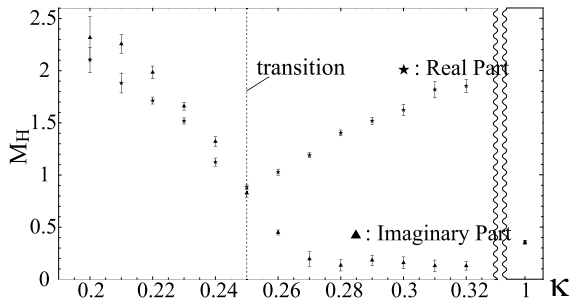


FIG. 7. Masses $M_H(N = 16)$ of real and imaginary parts of $(\bar{\phi}_{x+\mu} U_{x\mu} \phi_x)$ vs. κ for $g = 0.4$. M_H of the real part has its minimum at the transition point as in the 4D local AHM.

-
- [1] See, for example, T.Senthil, V.Vishwanath, L.Balents, S.Sachdev, and M.P.A.Fisher, *Science* **303**, 1490(2004).
 - [2] P.W.Anderson, *Phys.Rev.Lett.* **64**,1839(1990).
 - [3] J.K.Jain, *Phys.Rev.Lett.* **63**, 199(1989).
 - [4] I.Ichinose and T.Matsui, *Nucl.Phys.* **B394**, 281(1993); *Phys.Rev.* **B51**, 11860(1995); I.Ichinose and T.Matsui, and M.Onoda, *Phys.Rev.* **B64**, 104516(2001).
 - [5] I.Ichinose and T.Matsui, *Phys.Rev.* **B68**, 085322(2003).
 - [6] A.M.Polyakov, *Nucl.Phys.* **B120**, 429(1977).
 - [7] C.Nayak, *Phys.Rev.Lett.* **85**, 178(2000); I.Ichinose and T.Matsui, *Phys.Rev.Lett.* **86**, 942(2001); N.Nagaosa, *Phys.Rev.Lett.* **71**,4210(1993); H.Kleinert, F.S.Nogueira, and A.Sudbø, *Phys.Rev.Lett.* **88**, 232001 (2002); *Nucl.Phys.* **B666**, 361(2003); B.Børkje, S.Kragset, and A.Sudbø, *Phys.Rev.Lett.* **92**,186403 (2004); *Phys.Rev.* **B71**, 085112(2005); I.F.Herbut and B.H.Seradje, *Phys.Rev.Lett.* **91**,171601 (2003); I.F.Herbut, B.H.Seradje, S.Sachdev, and G.Murthy, *Phys.Rev.* **B68**, 195110 (2003).
 - [8] G.Arakawa, I.Ichinose, T.Matsui, and K.Sakakibara, *Phys.Rev.Lett.* **94**, 211601(2005); G.Arakawa, I.Ichinose, T.Matsui, K.Sakakibara, and S.Takashima, *Nucl.Phys.* **B732**, 401 (2006).
 - [9] For Dirac fermions without parity invariance, the Chern-Simons term may be generated. See Sect.2.3 of the second reference of Ref. [8].
 - [10] I.Affleck and B.Marston, *Phys.Rev.* **B37**,3774(1988).
 - [11] W.Rantner and X.-G.Wen, *Phys.Rev.Lett.* **86**, 3871 (2001); M.Hermele, T.Senthil, and M.P.A.Fisher, *cond-mat/0502215*.
 - [12] M.N.Chernodub, E.-M.Ilgenfritz, and A.Schiller, *Phys. Lett.* **B547**, 269(2002).
 - [13] S.Wenzel, E.Bittner, W.Janke, A.M.J.Schakel, and A.Schiller, *Phys.Rev.Lett.* **95**, 051601(2005).
 - [14] Strictly speaking, a term of Polyakov lines, $A_{PL} = g \sum_{x,i,\tau} c_{N_0}(P_x + \bar{P}_x)$, $P_x \equiv \prod_{\tau} U_{x+\tau\hat{0},0}$ is to be added to A_G . This term works as an external field to violate the global symmetry $\theta_{x0} \rightarrow \theta_{x0} + \alpha$. We performed separate simulations and checked that inclusion of this term does not affect the phase structure presented in the present paper.
 - [15] See, for example, J.M.Thijssen, “*Computational Physics*” (Cambridge University Press, 1999).
 - [16] E.Fradkin and S.Shenker, *Phys.Rev.* **D19**,3682 (1979).
 - [17] T.A.DeGrand and D.Toussaint, *Phys.Rev.* **D22**,2478 (1980); R.J.Wensley and J.D.Stack, *Phys.Rev.Lett.* **63**, 1764(1989).
 - [18] M.B.Einhorn and R.Savit, *Phys.Rev.* **D19**, 1198(1979).
 - [19] For accurate estimation of M_H , see S.Takashima, I.Ichinose, and T.Matsui, *Phys. Rev.* **B72**, 075112(2005).
 - [20] H.G.Evertz, K.Jansen, J.Jersák, C.B.Lang, and T.Neuhaus, *Nucl.Phys.* **B285**, 590(1987).